INVITED PAPER *Special Section on Recent Progress in Measurement and Design Techniques on Antennas, Propagation and Wireless Systems*

S-Parameter Method and Its Application for Antenna Measurements

Takayuki SASAMORI[†a)], ***Senior Member and*** **Toru FUKASAWA**[††], ***Member***

SUMMARY This paper focuses on the S-parameter method that is a basic method for measuring the input impedance of balanced-fed antennas. The basic concept of the method is summarized using the two-port network, and it is shown that the method can be enhanced to the unbalanced antennas using a formulation based on incident and reflected waves. The compensation method that eliminates the influence of a measurement jig and the application of the S-parameter method for the measurement of a radiation pattern with reduced unbalanced currents are explained. Further, application of the method for measuring the reflection and coupling coefficients of multiple antennas is introduced. The measured results of the input impedance of a dipole antenna, radiation patterns of a helical antenna on a small housing, and S-parameters of multiple antennas on a small housing are examined, and the measured results obtained with the S-parameter method are verified.

key words: *S-parameter method, input impedance, radiation pattern, reflection coefficient*

1. Introduction

The S-parameter method was proposed by Meys in 1998 to measure the impedance characteristics of a balanced-fed antenna [1]. Because most measurement systems employ unbalanced lines such as a coaxial cable, a balun is required to measure the characteristics of a balanced-fed antenna. A balun works as a transformer between a balanced line and an unbalanced line. If a balanced antenna is measured without a balun, a measurement error occurs owing to the unbalanced current induced on the outside of the coaxial cable. Generally, a balun has limited bandwidth, and the frequency characteristics of the balun must be considered in measurements. Therefore, the measurement of the pure impedance of a balanced fed-antenna is difficult. The S-parameter method enables measurement of '*the pure impedance*' by synthesizing the balanced mode impedance from the measurements of S-parameters of two ports. In actual measurements, two unbalanced lines (microstrip lines in [1]) are connected to each element of a dipole antenna. The S-parameter method can be easily applied because it requires only a simple jig composed of two unbalanced lines.

After Meys, Palmer proposed the utilization of coaxial cables in a jig and expanded the upper limit of measurement frequency [2]. Palmer's jig contributed to the popularization of the S-parameter method for small antenna measurements. This method has been applied to a symmetric antenna such as a dipole antenna [1], [2], a bowtie antenna [2], [3], a modified dipole antenna [4], [5], an antenna integrated with a circuit [6], [7], and a patch antenna with two orthogonal modes [8]. Applications for measurement of Radio Frequency IDentification (RFID) tag antennas are especially popular. RFID tags are composed of printed antennas on film circuit boards with IC chips mounted on them. In these cases, antenna elements themselves become RFID tags. The S-parameter method can be successfully applied to these kinds of antennas [9]–[15].

Further, the S-parameter method can also be applied to an asymmetric antenna. For an asymmetric antenna, balanced feeding satisfies only the necessary condition (i.e., only balanced feeding is not sufficient) for reducing the effect of feeding cable. The sufficient condition to reduce the influence of a feeding cable requires blocking effect against unbalanced current, namely, a high impedance for the unbalanced current [16]. The S-parameter method satisfies the latter condition by itself. Namely, by applying the S-parameter method to an asymmetric antenna, the unbalanced current on a measurement cable can be reduced and the measurement accuracy can be improved. For example, an asymmetric antenna was measured by using the S-parameter method and accurate results were shown for a wide range of bandwidths in [17]. An offset fed dipole antenna [18], RFID tags with asymmetric configurations [10], [12], [13], [18], and an antenna on a small housing [19] were also measured successfully by using the S-parameter method.

Moreover, the S-parameter method has also been improved continuously. The method requires a jig composed of two unbalanced feed lines such as coaxial cables or microstrip lines. The jig must be calibrated to achieve accurate results especially at high frequencies. For semi-rigid coaxial cables, a correction method by using shorted end [2] and shorted and open ends [20] are proposed. However, these methods can only correct the electrical delay of a jig and cannot overcome the reflection effect between a jig and a measurement cable, on which SOLT calibration is based. To overcome the above problem, the TRL method has been proposed in [21]. Accurate measurement results for high frequencies, above 10 GHz, can be obtained with the TRL method that removes the reflection effect.

Radiation patterns can also be measured by using the S-parameter method [22]. The ratio of excitation coefficients

Manuscript received February 4, 2014.
Manuscript revised May 12, 2014.

[†]The author is with Akita Prefectural University, Yurihonjo-shi, 015-0055 Japan.
[††]The author is with Mitsubishi Electric Corporation, Kamakura-shi, 247-8501 Japan.
a) E-mail: sasa@akita-pu.ac.jp

DOI: 10.1587/transcom.E97.B.2011

of two cables, under the condition where unbalanced current of coaxial cables is canceled at antenna feed point, are calculated uniquely from S-parameters. As the special case, the ratio equals -1 for symmetric antennas, that is same amplitude and opposite phase [15], [23]. The active impedance for the above excitation ratio is the same as the differential input impedance shown in [1] and [24]. Therefore, the S-parameter method certainly guarantees blocking of the unbalanced current even for an asymmetric antenna. The radiation pattern obtained by using an array pattern with the above excitation coefficients has reduced influence of measurement cables. The concept of exciting two cables to reduce the unbalanced current can also be extended to the measurement of the reflection and coupling coefficients of multiple antennas [25].

Recently, a quantitative analysis of balanced and unbalanced modes for antennas with symmetric and asymmetric configurations has been proposed in [24], [26], [27]. A concept of mixed mode S-parameter is adopted and its relationship with the S-parameter method is discussed in [24], [28]. Further, a combination of the S-parameter method and the Wheeler cap method was proposed to measure the efficiency of a small antenna supported in air in [29] whereas the conventional Wheeler cap method can be applied only for an antenna mounted on the surface of a large ground plane.

As mentioned above, the S-parameter method has been applied to measure not only the impedance but also the radiation patterns, efficiency, and coupling between antennas. It is also used to explain the balanced and unbalanced phenomena and can be applied in a wider area of measurements. This paper summarizes the basics and applications of the S-parameter method. In Sect. 2, we introduce the formulations of the S-parameter method based on the two-port network and the incident and reflected waves concept. In Sect. 3, the calibration method of a measurement jig, radiation pattern measurement, and application to measurement of multiple antennas are described. Finally, measurement results and conclusions are given in Sects. 4 and 5, respectively.

2. Formulation of S-Parameter Method

Figure 1 shows the measurement model for the S-parameter method. The configuration of an antenna does not have to be symmetric. A type of a monopole antenna on a housing, in which one element of the antenna is a monopole and the other is a ground plane, is also acceptable. The output ports of the coaxial cables connected to each element are denoted as port 1 and port 2, respectively. The incident and reflected waves in each port are defined as a_1 and a_2 and b_1 and b_2, respectively. Moreover, the voltages from the outer conductor to the inner conductor are defined as V_1 and V_2, respectively. The currents on the inner conductor are defined as I_1 and I_2, respectively. The condition under which the currents on the outside of the two coaxial cables (unbalanced current) cancel each other is expressed below.

$$I_1 = -I_2 \tag{1}$$

The basic idea of the S-parameter method is to extract the impedance characteristics from full two ports S-parameters ($S_{11}, S_{12}, S_{21}, S_{22}$) under the condition of Eq. (1).

Initially, the derivation of the S-parameter method based on the two-port network is explained. Thereafter, the formulation based on incident and reflected waves is described.

2.1 Formulation Based on Two-Port Network

Using the impedance matrix of the two-port network, as shown in Fig. 2, the equation for the balanced-fed antenna is given by

$$\begin{cases} V_1 = Z_{11}I_1 + Z_{12}I_2 \\ V_2 = Z_{21}I_1 + Z_{22}I_2 \end{cases}. \tag{2}$$

When the antenna is fed by a balanced source, the currents flowing on the two radiation elements are $I = I_1 = -I_2$ (shown in Eq. (1)). Because the differential voltage is $V_d = V_1 - V_2$, the input impedance (Z_{in}) is expressed using the Z-parameter as below.

$$Z_{in} = \frac{V_d}{I} = Z_{11} - Z_{21} - Z_{12} + Z_{22} \tag{3}$$

By converting the Z-parameter into an S-parameter, the input impedance can be written as [30]

$$Z_{in} = 2R_0 \frac{(1 - S_{12})(1 - S_{21}) - S_{11}S_{22}}{(1 - S_{11})(1 - S_{22}) - S_{12}S_{21}}, \tag{4}$$

where R_0 is the characteristic impedance of the coaxial cables. Equation (4) is generally called the S-parameter method and is used for the measurement of balanced impedance [1]. In addition, it can be converted into an

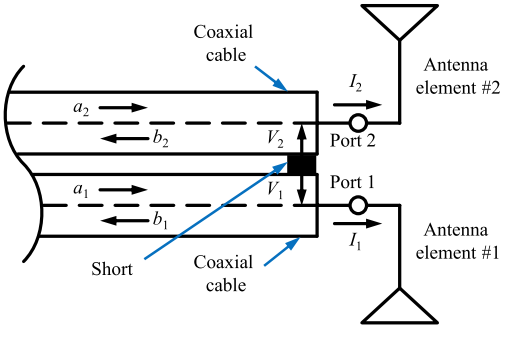

Fig. 1 Measurement model for S-parameter method.

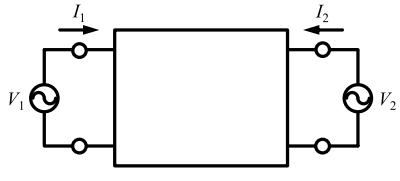

Fig. 2 Two-port network.

ABCD-parameter as follows:

$$Z_{in} = \frac{1}{C}(A + D - AD + BC - 1). \tag{5}$$

The balanced-fed antenna has symmetric geometry, and the two-port network is a symmetric circuit ($Z_{11} = Z_{22}$, $S_{11} = S_{22}$, $A = D$) and a reciprocal circuit ($Z_{12} = Z_{21}$, $S_{12} = S_{21}$, $AD - BC = 1$). Therefore, Eqs. (3)–(5) can be reduced to

$$Z_{in} = 2(Z_{11} - Z_{21}), \tag{6}$$

$$Z_{in} = 2R_0\frac{1 + S_{11} - S_{21}}{1 - S_{11} + S_{21}}, \tag{7}$$

$$Z_{in} = \frac{2}{C}(A - 1). \tag{8}$$

2.2 Formulation Based on Incident and Reflected Waves

The S-parameter method explained in Sect. 2.1 is based on the two-port network [1], [2]. In this section, a formulation based on incident and reflected waves that can be easily extended to radiation patterns or multi-port measurements is discussed [22].

The incident waves, reflected waves, and S-parameters are related as follows:

$$\begin{aligned} b_1 &= S_{11}a_1 + S_{12}a_2 \\ b_2 &= S_{21}a_1 + S_{22}a_2 \end{aligned} \tag{9}$$

If the characteristic impedance is normalized to 1, the currents I_1 and I_2 can be expressed as follows:

$$I_i = a_i - b_i \quad (i = 1, 2) \tag{10}$$

From Eqs. (1) and (10), we obtain the following relationship:

$$a_1 + a_2 = b_1 + b_2 \tag{11}$$

If b_1 and b_2 are eliminated from Eq. (9), the following equations can be obtained:

$$a_2 = -\frac{1 - S_{11} - S_{21}}{1 - S_{22} - S_{12}}a_1 = \alpha a_1 \tag{12}$$

$$\alpha \equiv -\frac{1 - S_{11} - S_{21}}{1 - S_{22} - S_{12}} \tag{13}$$

Equation (12) implies that if both ports are excited with a ratio α, the unbalanced current at the feed point of the antenna is canceled [satisfies Eq. (1)]. The physical interpretation is shown in Fig. 3. Figure 3(a) shows the condition where port 1 is fed, port 2 is terminated by the dummy load, and I_{u1} is assumed to be an unbalanced current on the outside of the coaxial cables. Figure 3(b) shows the condition where each port is interchanged and I_{u2} is assumed to be an unbalanced current. Both the ports are excited in a ratio of α, i.e., a_1 and $a_2 = \alpha a_1$, and each unbalanced current is canceled out at the feed point of the antenna, as shown in Fig. 3(c). In other words, a superposition of field F_1 (Fig. 3(a)) and α times of field F_2 (Fig. 3(b)) cancels the

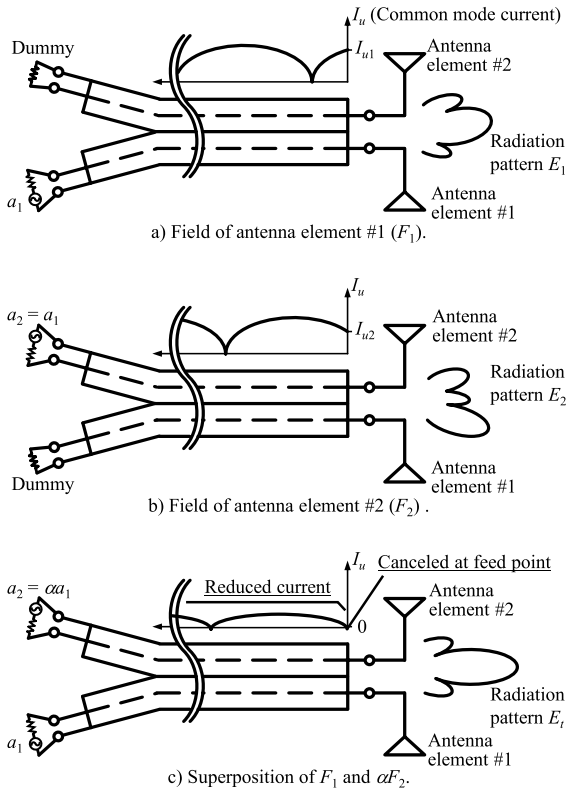

Fig. 3 Physical interpretation of S-parameter method.

unbalanced current. However, a zero unbalanced current is guaranteed only at the antenna feed point (at the outlet of each port). If the antenna is symmetric, and the cables are set in a symmetric plane, the unbalanced current is canceled all over the cables. If one of the above conditions is not satisfied, the unbalanced current exists except at the antenna feed point. Even in this case, the unbalanced current is significantly reduced when compared with the case where the cable is directly connected.

The reflection coefficients of each port in Fig. 3(c), S_1 and S_2, are given as Eq. (14).

$$\begin{cases} S_1 \equiv \dfrac{b_1}{a_1} = S_{11} - S_{12}\dfrac{1 - S_{11} - S_{21}}{1 - S_{22} - S_{12}} \\ S_2 \equiv \dfrac{b_2}{a_2} = S_{22} - S_{21}\dfrac{1 - S_{22} - S_{12}}{1 - S_{11} - S_{21}} \end{cases} \tag{14}$$

The impedance Z_n between the antenna elements #1 and #2 is obtained as a series combination of Z_1 and Z_2, where Z_1 and Z_2 are the impedances that give the reflection coefficients S_1 and S_2, respectively, in Eq. (14).

$$\begin{aligned} Z_n &= Z_1 + Z_2 = R_0\left(\frac{1 + S_1}{1 - S_1} + \frac{1 + S_2}{1 - S_2}\right) \\ &= 2R_0\frac{(1 - S_{12})(1 - S_{21}) - S_{11}S_{22}}{(1 - S_{11})(1 - S_{22}) - S_{12}S_{21}} \end{aligned} \tag{15}$$

This is the desired impedance Z_n when the unbalanced currents on the outside of the coaxial cables are canceled. It can be understood that Eq. (15) completely equals to (4). If we

assume that the antenna has a symmetric structure, such as a dipole ($S_{11} = S_{22}$, $S_{12} = S_{21}$), Eq. (7) is also obtained and it equals the differential input impedance given in [1] and [24].

3. Application and Extension of S-Parameter Method

Though the basic concept and formulations for accurate impedance measurement have been described in the Sect. 2, the influence of the jig on the measurement results becomes significant as the frequency increases. Moreover, conventional method has been applied only for impedance measurement with one port. The compensation method for the jig using the ABCD-parameter and the measurement methods for radiation patterns and multiple antennas are expounded as applications of the S-parameter method.

3.1 Calibration Method of a Measurement Jig

Figure 4 shows an example of a system for measurement of input impedance of a balanced antenna. Each port of the balanced antenna is connected to one of the ports of the VNA using a measurement jig. The measurement jig is composed of jigs #1 and #2.

Two basic types of jigs have been reported: one made of coaxial cables, as shown in Fig. 5(a), [2], [3], [5] and the other is comprised of a microstrip line, as shown in Fig. 5(b) [1], [21]. When the VNA is calibrated at the connector of the coaxial cable using the SOLT calibration technique, port extension or ABCD-matrix compensation such as the open-correction method (described later) is used to extend the measurement reference plane to the end of the jig. On the other hand, for a jig made of a microstrip line, the calibration plane can also be directly at the end of the jig using the TRL calibration technique.

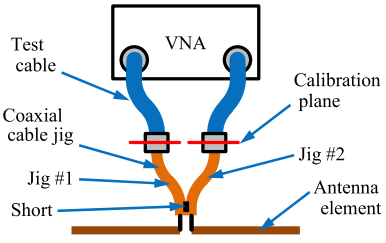

Fig. 4 Measurement system for input impedance of balanced antenna.

a) Coaxial cable type.

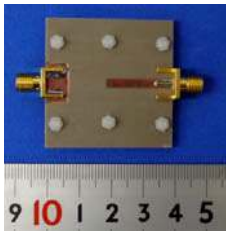

b) Microstrip line type.

Fig. 5 Examples of measurement jigs.

In order to eliminate the effect of the jig, a compensating method involving the ABCD-matrix is used. Figure 6 shows the circuit diagram of an antenna connected to a jig for measurement in a two-port network configuration. The ABCD-matrix (K') that is between the calibration planes can be determined by substituting the S-parameter in Eq. (16).

$$\mathrm{K'} = \begin{bmatrix} \dfrac{(1+S_{11})(1-S_{22})+S_{12}S_{21}}{2S_{21}} & \dfrac{(1+S_{11})(1+S_{22})-S_{12}S_{21}}{2S_{21}} \\ \dfrac{(1-S_{11})(1-S_{22})-S_{12}S_{21}}{2S_{21}} & \dfrac{(1-S_{11})(1+S_{22})+S_{12}S_{21}}{2S_{21}} \end{bmatrix} \tag{16}$$

As shown in Fig. 6, the characteristics of the jigs are included in K', and K of the antenna can be obtained by removing the influence of jigs #1 and #2, as given by

$$\mathrm{K} = \mathrm{K}_{\mathrm{J1}}^{-1}\,\mathrm{K'}\,\mathrm{K}_{\mathrm{J2}}^{-1}. \tag{17}$$

Here, K_{J1} and K_{J2} are the ABCD-matrices of jigs #1 and #2. Conclusively, the input impedance of the balanced antenna can be obtained when the ABCD-parameter of matrix K is substituted in Eq. (5).

Four types of compensation techniques using the ABCD-matrix referred to as open-correction, short-correction, open-short-correction and modified open-correction methods that express the characteristics of the measurement jig are explained. Similarly, K_{J1} and K_{J2} can be derived.

The open- and short-correction methods are used to determine the ABCD-parameter of the jig using the input impedance of the jig terminated in an open circuit and a short circuit, respectively, and the characteristic impedance of the transmission line to use for the jig. At the calibration plane, the input impedance Z_{in} looking toward the load impedance Z is

$$Z_{in} = Z_0 \frac{Z + Z_0 \tanh \gamma l}{Z_0 + Z \tanh \gamma l}, \tag{18}$$

where Z_0, γ, and l denote the characteristic impedance, propagation constant, and length of the transmission line, respectively. $Z = \infty$ and $Z = 0$ are substituted in Eq. (18) for open-correction and short-correction methods, respectively. Therefore, for both the cases, the input impedance of the jig at the calibration plane can be given by

$$\begin{cases} Z_{Open} = Z_0/\tanh \gamma l : & \mathrm{open-circuit} \\ Z_{Short} = Z_0 \tanh \gamma l : & \mathrm{short-circuit} \end{cases}, \tag{19}$$

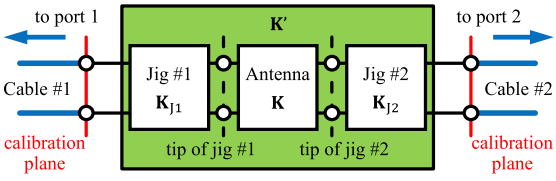

Fig. 6 Equivalent circuit diagram of antenna with jig.

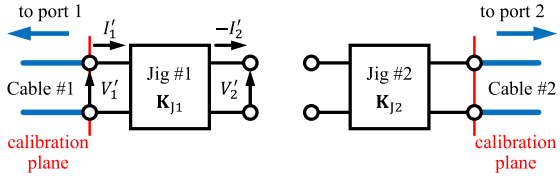

Fig. 7 Circuit diagram of measurement jig for open-short-correction.

where Z_{Open} and Z_{Short} are the input impedances at the calibration plane for the open and short circuited lines, respectively. The hyperbolic functions $\sinh \gamma l$ and $\cosh \gamma l$ can be given by $\cosh^2 \gamma l - \sinh^2 \gamma l = 1$ and Eq. (19). Consequently, the ABCD-matrix of the jig can be written as

$$\begin{cases} \mathrm{K_J} = \dfrac{1}{\sqrt{Z_{Open}^2 - Z_0^2}} \begin{bmatrix} Z_{Open} & Z_0^2 \\ 1 & Z_{Open} \end{bmatrix} : & \text{open - correction} \\ \mathrm{K_J} = \dfrac{1}{\sqrt{Z_0^2 - Z_{Short}^2}} \begin{bmatrix} Z_0 & Z_0 Z_{Short} \\ \frac{Z_{Short}}{Z_0} & Z_0 \end{bmatrix} : & \text{short - correction} \end{cases}. \tag{20}$$

Next, the open-short-correction method is used for determining the ABCD-matrix of the jig as shown in Fig. 7, using both the input impedances of the open- and short-circuited lines. When the jig is expressed by the ABCD-matrix, the input impedance Z at the calibration plane is given by

$$Z = \frac{V_1'}{I_1'} = \frac{AV_2' + BI_2'}{CV_2' + DI_2'}. \tag{21}$$

When the jig is terminated in an open circuit, $I_2' = 0$. Then, from Eq. (21), the input impedance for the open circuit is $Z_{Open} = A/C$. Similarly, when the jig is terminated in a short circuit, $V_2' = 0$, and the input impedance for the short circuit is $Z_{Short} = B/D$. Because the jig is a symmetrical circuit ($A = D$) and a reciprocal circuit ($AD - BC = 1$), the ABCD-matrix $\mathrm{K_J}$ is given by

$$\mathrm{K_J} = \sqrt{\frac{Z_{Open}}{Z_{Open} - Z_{Short}}} \begin{bmatrix} 1 & Z_{Short} \\ 1/Z_{Open} & 1 \end{bmatrix}. \tag{22}$$

Although the load impedance is assumed to be infinite in the derivation of open-correction, it actually has a finite value. We propose a modified open-correction method that considers the influence of the load impedance Z. The ABCD-matrix compensating the influence of the impedance at the open end of the jig is given by Eq. (23) from Eq. (18).

$$\mathrm{K_J} = \frac{1}{\sqrt{\left(Z^2 - Z_0^2\right)\left(Z_{Open}^2 - Z_0^2\right)}} \begin{bmatrix} Z_{Open}Z - Z_0^2 & Z_0^2\left(Z - Z_{Open}\right) \\ Z - Z_{Open} & Z_{Open}Z - Z_0^2 \end{bmatrix} \tag{23}$$

3.2 Measurement Method for Radiation Patterns

Section 2.2 explains that the superposition of field F_1, obtained by feeding port 1, and α times of field F_2, obtained by feeding port 2, produces a measurement with canceled unbalanced currents. This concept can be readily applied to the measurement of radiation patterns [22]. Let us define E_1 and E_2 as the array-element patterns for antenna elements #1 and #2, respectively. E_1 and E_2 correspond to the radiation patterns of fields F_1 and F_2, shown in Fig. 3, respectively. The measurement system for radiation pattern E_1 is shown in Fig. 8. Further, E_1 is measured with the transmission coefficient between two ports of a VNA. To obtain E_2, the cable connected to one antenna element is reconnected to the other antenna. During the measurement, the disconnected port of the antenna under test must be terminated by a dummy load.

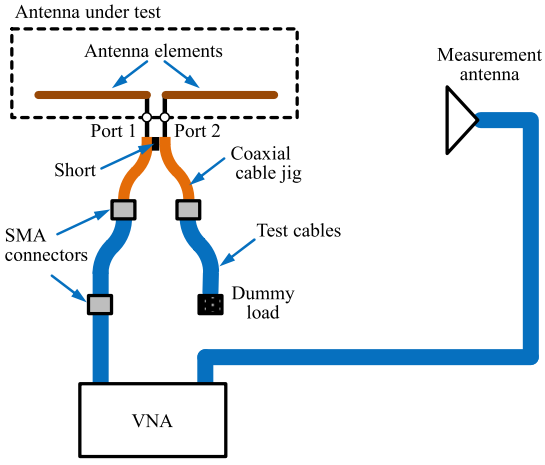

Fig. 8 Measurement system for radiation pattern E_1.

The synthesized array pattern (E_t) obtained with the following equation implies that it is a radiation pattern with a canceled unbalanced current on the outside of the coaxial cables.

$$E_t = E_1 + \alpha E_2 \tag{24}$$

Here, E_t corresponds to the measured radiation pattern under the condition of Fig. 3(c). Although the idea of offline synthesis of array-element patterns is also presented in [23], it is valid only for a symmetric antenna, i.e., for $\alpha = -1$ in Eq. (24). A combination of Eqs. (13) and (24) is more general and valid even for an asymmetric antenna.

When the two ports are excited by a_1 and αa_1, the reflected waves b_1 and b_2 can be given as follows:

$$\begin{cases} b_1 = (S_{11} + S_{12}\alpha)\, a_1 \equiv \beta a_1 \\ b_2 = (S_{21} + S_{22}\alpha)\, a_1 \equiv \gamma a_1 \end{cases} \tag{25}$$

Subtracting the reflected power from the incident power for both the ports results in the total incident power (P_{in}).

$$\begin{aligned} P_{in} &= |a_1|^2 + |a_2|^2 - |b_1|^2 - |b_2|^2 \\ &= |a_1|^2 \left(1 + |\alpha|^2 - |\beta|^2 - |\gamma|^2\right) \end{aligned} \tag{26}$$

If a standard gain antenna with a gain of G_d is connected to port 1, the input power (P_{ind}) to the antenna be-

comes $P_{ind} = |a_1|^2$. If E_d is the observed level for the standard gain antenna, the absolute gain (G_a) of the antenna under test can be expressed as below.

$$G_a = \frac{|E_t|^2 / P_{in}}{|E_d|^2 / G_d P_{ind}} = G_d \frac{|E_t|^2}{|E_d|^2 \left(1 + |\alpha|^2 - |\beta|^2 - |\gamma|^2\right)} \tag{27}$$

Further, G_a divided by the mismatch loss (M, positive in dB) results in the actual gain (G_{act}), which can be expressed as follows:

$$G_{act} = \frac{G_a}{M} = G_a \left(1 - \left|\frac{Z_n - R_0}{Z_n + R_0}\right|^2\right) \tag{28}$$

3.3 Measurement Method for Multiple Antennas

In this section, the application of the S-parameter method for the measurement of reflection and coupling coefficients of multiple antennas is described. If the number of antennas is assumed to be n, a measurement of $2n$ ports is required to apply the S-parameter method. Equation (9) is rewritten as below.

$$\mathbf{B} = \mathbf{SA} \tag{29}$$

Here, $\mathbf{A}$ and $\mathbf{B}$ are the incident and reflected wave vectors for each port and are composed of $2n$ elements each. $\mathbf{S}$ is a scattering matrix of size $2n \times 2n$.

The balance conditions at the feed point of each antenna are given as follows:

$$i_{2k-1} = -i_{2k} \quad (k = 1, 2, \ldots, n) \tag{30}$$

When the coupling from the mth antenna to other antennas ($S_{1m}, S_{2m}, \ldots, S_{nm}$) are to be measured, the other antennas must be terminated by dummy loads ($a_i = 0$; $i = 1, 2, \ldots n$; $i \neq m$). Under these conditions,

$$-a_{2k-1} + 2a_{2k} - b_{2k-1} = 0 \quad (k = 1, 2, \ldots, n. \quad k \neq m) \tag{31}$$

From Eqs. (29), (30), and (31), $4n - 1$ conditions are obtained. Because Eq. (29) has an unknown $4n$ element ($a_1, \ldots, a_{2n}, b_1, \ldots, b_{2n}$), we can solve the system of equations by normalizing other unknowns using one certain unknown. Here, we choose a_{m-1} as the '*certain unknown*' that normalize other unknowns. The symbol $\hat{}$ represents the unknown is normalized one. The incident and reflected waves at the antenna feed point can be calculated with the elements of vectors $\mathbf{A}$ and $\mathbf{B}$. When the mth antenna is excited, the reflection coefficient S_{mm}, and the coupling from port m to port k, S_{km}, are provided by the following equations [25]:

$$S_{m,m} = \frac{-1 - \hat{b}_{2m-1} + 2\hat{b}_{2m}}{-1 + 2\hat{a}_{2m} - \hat{b}_{2m-1}} \quad (m = 1, 2, \ldots, n) \tag{32}$$

$$S_{k,m} = \frac{-\hat{a}_{2k-1} - \hat{b}_{2k-1} + 2\hat{b}_{2k}}{-1 + 2\hat{a}_{2m} - \hat{b}_{2m-1}} \quad (m = 1, 2, \ldots, n. \quad k = 1, 2, \ldots, n. \quad m \neq k) \tag{33}$$

4. Measurement Results

In this section, the measured results of the input impedance of a dipole antenna, radiation patterns of a helical antenna on a small housing, and S-parameters of a multiple antenna system on a small housing are examined, and the measured results of the S-parameter method are verified.

4.1 Input Impedance of Dipole Antenna

We will first discuss the measured input impedance of the dipole antenna shown in Fig. 9. The total length of the dipole antenna is 200 mm, and the diameter of the radiation element is 0.35 mm. The measurement jig is made of coaxial cables, as shown in Fig. 5(a). For verifying the effectiveness of the open-correction, short-correction, and open-short-correction methods, the experimental result of a monopole antenna on an aluminum plate of $1.25 \times 1.25\ \mathrm{m}^2$ is also shown. The measured result of the monopole antenna is doubled so as to compare it with that of a dipole antenna. It can be seen that the measured results of the S-parameter method agree well with the result of the monopole antenna. Some sharp peak-shaped errors are caused by the input impedance of the jig terminated in an open circuit, and a short circuit becomes infinite. Additionally, as can be seen, there is a slight resonance frequency shift. The frequency

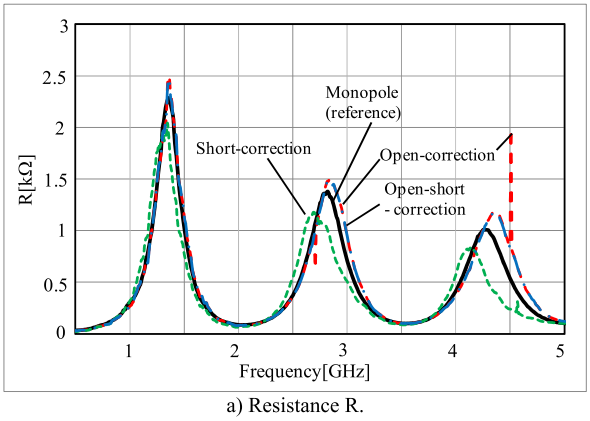

a) Resistance R.

b) Reactance X.

Fig. 9 Measured input impedance of dipole antenna.

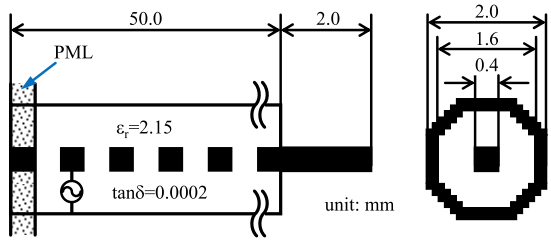

Fig. 10 Calculated model of open-end jig made of coaxial cable.

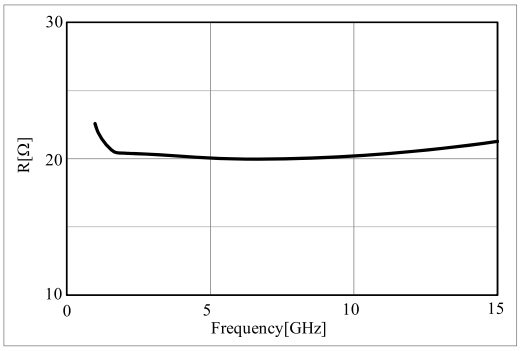

a) Resistance R.

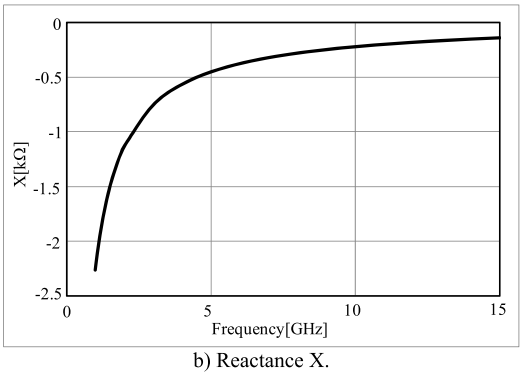

b) Reactance X.

Fig. 11 Calculated load impedance at open end of the jig.

shift of the open-correction is discussed in the following paragraph.

In order to improve the accuracy of measurement of the open-correction method, the modified open-correction method that considers the influence of the load impedance at the open end of the jig is examined. The load impedance at the open end of the coaxial cable is calculated by using the FDTD method. Figure 10 shows an FDTD model of an RG405 coaxial cable. The inner conductor is longer than the outer conductor by 2 mm to connect the antenna element. This numerical model is considered to be valid because the calculated value of the characteristic impedance of this coaxial cable is $Z_0 = 49.3 - j0.136\,\Omega$. Figure 11 shows the load impedance at the open end of the coaxial cable. The load resistance and the load reactance are 20.1 Ω and −447.7 Ω, respectively at a frequency of 5 GHz.

Figure 12 shows an FDTD model of a dipole antenna for obtaining the input impedance. Figures 12(a) and 12(b)

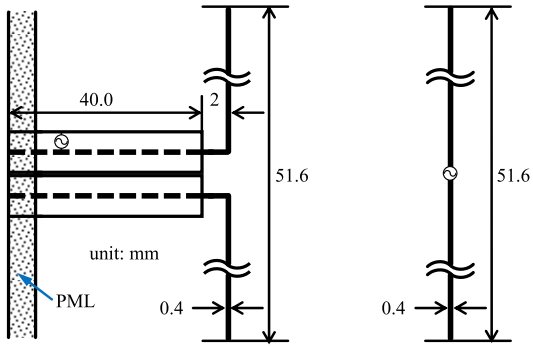

a) S-parameter method. b) Conventional model.

Fig. 12 Calculated model of dipole antenna.

show the dipole elements with a measurement jig for the S-parameter method and a conventional dipole antenna model with a delta gap feed, respectively. The total length of the dipole antenna is 51.6 mm by shortage of the calculation ability of used PC, and the section of the elements is a square of $0.4 \times 0.4\,\text{mm}^2$ for both the calculation models. It is confirmed that the length of the coaxial cable of the jig is long enough by the calculation that changes the length of the cable.

Figure 13 shows the calculated input impedance of the dipole antenna using the S-parameter method and the conventional model. The results of the open-correction and the modified open-correction methods are shown for the S-parameter method. As can be seen, the resonance frequency of the open-correction method shifts from that of the conventional model, and the peak values are different. In the case of the modified open-correction method, it can be seen that the result is somewhat in agreement with the result of the conventional model. Further, as can be seen, the load impedance of the open end of the measurement jig influences the measured value. The input impedance without correction is also shown for a comparison. It is understood that it does not agree with the reference value at all.

4.2 Measurement Results for an Antenna on a Small Housing

In this section, application of the S-parameter method for measuring an antenna on a small housing is explained [22]. Figure 14 shows the measurement model. Because the size of the housing is much smaller than the wavelength of the operation frequency (315 MHz), the unbalanced current is significant when a measurement cable is connected directly. Therefore, the measurement results have a large error if the conventional measurement method is applied. The S-parameter method can significantly improve the measurement accuracy for this type of antennas.

As a measurement model, a helical antenna element with a square cross section of $10\times10\,\text{mm}^2$ and 28 mm length is mounted on a square housing ($40 \times 40\,\text{mm}^2$). The resonant frequency of the antenna is 315 MHz, and the total size

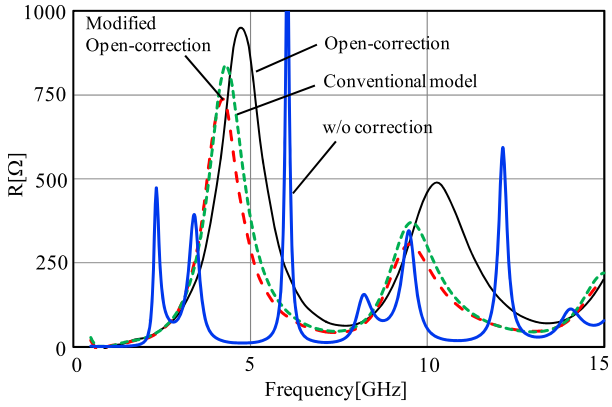

a) Resistance R.

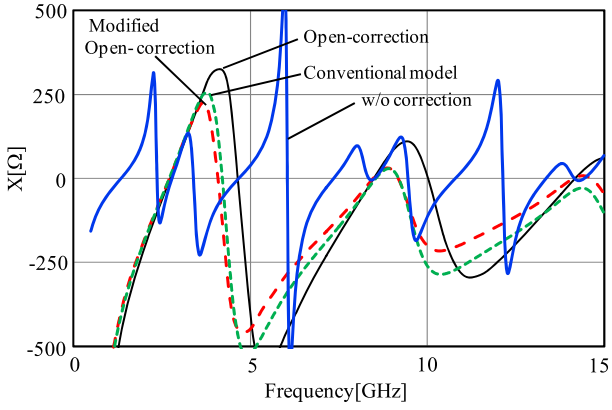

b) Reactance X.

Fig. 13 Calculated input impedance of dipole antenna.

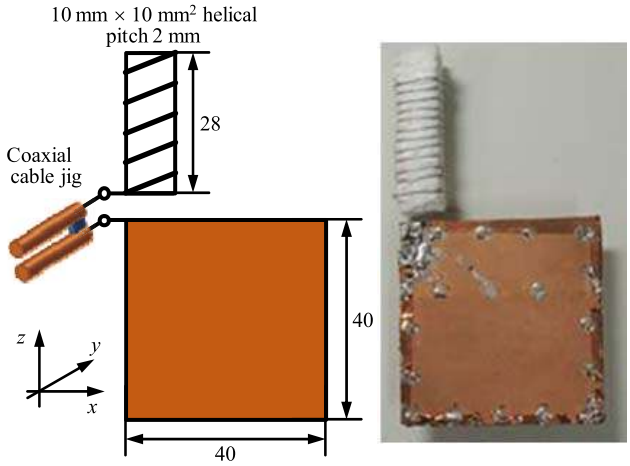

a) Configurations b) Manufactured model

Fig. 14 Measurement model for an antenna on a small housing.

of the antenna element and the housing is approximately $\lambda/14$. The impedance characteristics and radiation patterns are measured by using the S-parameter method. Ports 1 and 2, in Fig. 1, are connected to the housing and the antenna element, respectively.

Figures 15(a)–(c) show the measured S-parameters.

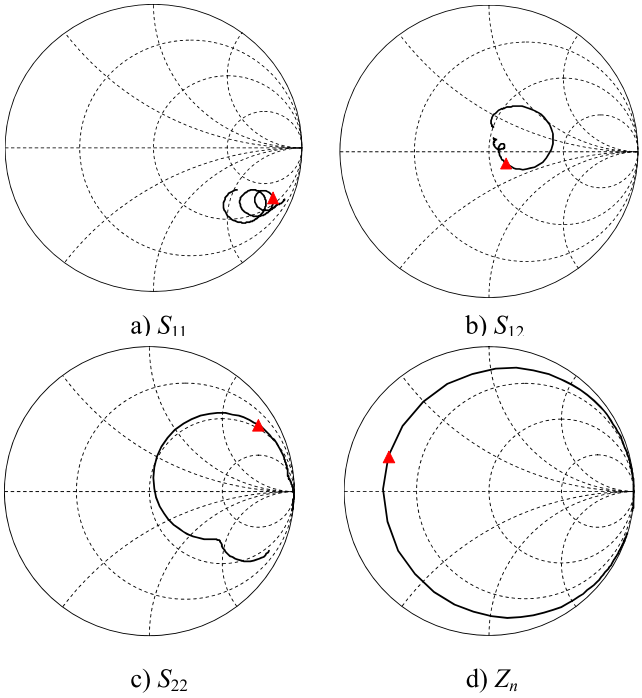

a) S_{11} b) S_{12}

c) S_{22} d) Z_n

Fig. 15 Measurement results for S-parameters and Z_n.

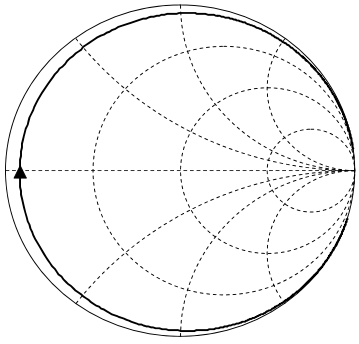

Fig. 16 Calculation result for antenna impedance (with PEC).

The markers are set at 315 MHz. Moreover, the impedance Z_n synthesized from the S-parameters using Eq. (15) is shown in Fig. 15(d). The calculated result of the antenna impedance is shown in Fig. 16.

Many kinks can be observed in Figs. 15(a)–(c). These are caused by the influence of the coaxial cables, where the S-parameter measurements are performed with a large unbalanced current on the outside of the coaxial cables (Fig. 3(a) or 3(b)). On the other hand, in Fig. 15(d), only single resonance characteristics without any kinks are observed thus demonstrating that the influence of the coaxial cables is reduced (Fig. 3(c)). As can be seen from Fig. 15(d) and Fig. 16, the measured and calculated results are in good agreement with each other. The error between them is mainly caused by conducting loss that is excluded from the calculation result. If the measurement cable is connected directly, the measurement result is almost same as that in Fig. 15(c). This fact shows that the result of conventional

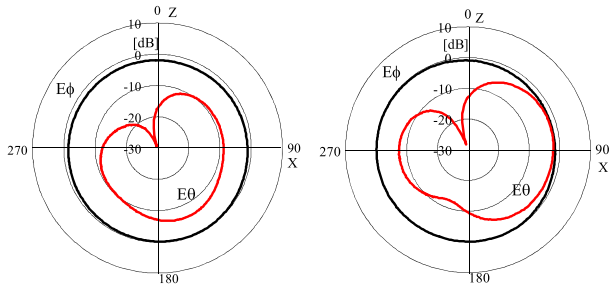

a) E_1 b) E_2

Fig. 17 Measurement results for E_1 and E_2.

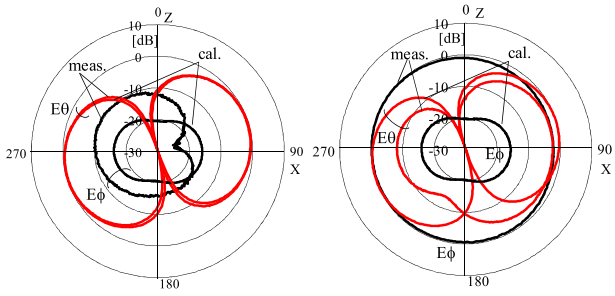

a) S-parameter method (E_t). b) Conventional method.

Fig. 18 Radiation patterns for S-parameter and conventional methods.

measurement method is quite different from calculated one.

Figures 17(a) and (b) show the radiation patterns of E_1 and E_2 in the ZX plane, respectively. In both the patterns, E_ϕ is greater than E_θ because the radiation from the unbalanced current on the outside of the coaxial cables is dominant (Fig. 3(a) or 3(b)). The pattern E_t synthesized by Eq. (24) is shown in Fig. 18(a). The calculated reference results without coaxial cables are also shown in the same figure. The undesired radiation from the coaxial cables is canceled (Fig. 3(c)), and the accuracy of the radiation pattern measurement is significantly improved. The measurement results with the coaxial cable connected directly, which is the conventional method, are shown in Fig. 18(b). The coaxial cable disturbs the measured radiation pattern and a pattern that is quite different from the reference pattern is observed.

The results of the S-parameter method for multiple antennas mounted on one small housing, that is the impedance characteristics (S_{11}) and mutual coupling (S_{21}) for the model of Fig. 19, are shown in Fig. 20. The measured frequency ranges from 700 MHz to 900 MHz, and the marker is set at 800 MHz. For comparison, the measurement results obtained with the conventional method (connecting coaxial cables directly) are also shown. Regarding reflection characteristics, the resonance frequency is drastically shifted from approximately 800 MHz to a lower frequency in the conventional method, and a correct measurement was not performed. Meanwhile, the results obtained with the proposed method are in good agreement with the calculated results,

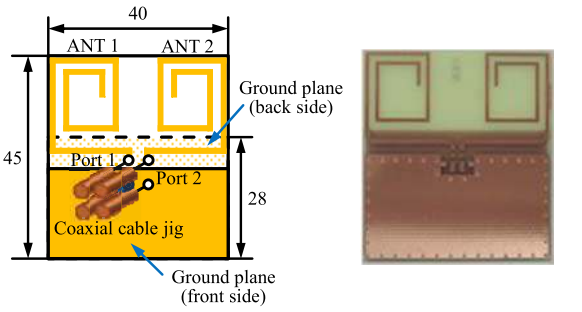

a) Configurations b) Manufactured model

Fig. 19 Measurement model for multiple antennas.

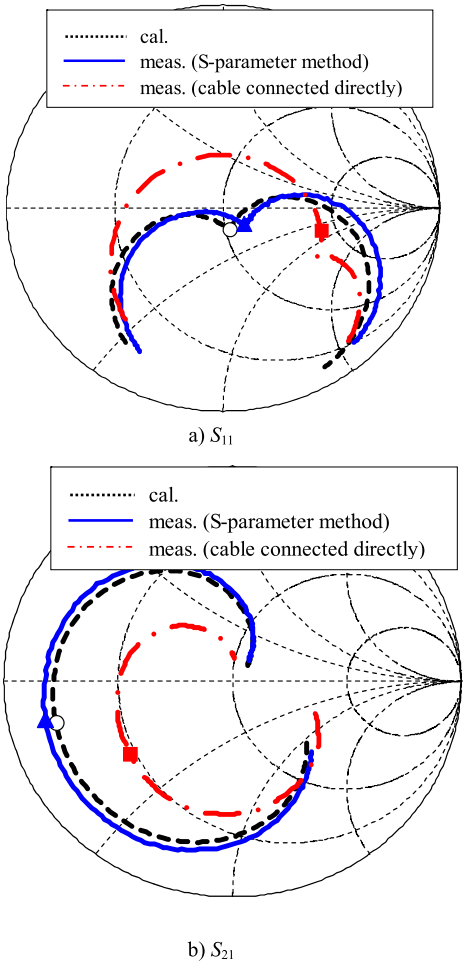

a) S_{11}

b) S_{21}

Fig. 20 Measurement results for multiple antennas.

and the measurement accuracy is improved.

5. Conclusion

In this paper, we have described the basic concept of the S-parameter method that is a basic method for measuring the input impedance of balanced-fed antennas and have proposed its application and extension. First, the formula-

tions of the S-parameter method based on the two-port network and the enhancement to the unbalanced antennas using a concept based on incident and reflected waves were described. Thereafter, a practical application that eliminates the influence of a measurement jig on the measurement of the input impedance in the high frequency range above 1 GHz and its extension to the measurement of radiation patterns of unbalanced antenna and a multi-port antenna were presented. Furthermore, to show the validity of the proposed approaches to measurement, the results of input impedances, S-parameters, and radiation patterns have been shown. It is notable that more accurate results of a measurement can be obtained by the proposed S-parameter method.

References

[1] R. Meys and F. Janssens, "Measuring the impedance of balanced antennas by an S-parameter method," IEEE Antennas Propag. Mag., vol.40, no.6, pp.62–65, Dec. 1998.
[2] K.D. Palmer and M.W. van Rooyen, "Simple broadband measurements of balanced loads using a network analyzer," IEEE Trans. Instrum. Meas., vol.55, no.1, pp.266–272, Feb. 2006.
[3] S. Konya, T. Sasamori, T. Tobana, and Y. Isota, "Wideband measurement of balanced antennas using the S-parameter method," Proc. IEICE Gen. Conf., B-1-226, March 2011. (in Japanese)
[4] E.B. Kaldjob, M.G. E. Din, B. Geck, and H. Eul, "A novel planar cylindrical waveguide-to-planar transition for transceivers at 2.45 GHz ISM-band," 2007 European Microw. Conf., pp.87–90, 2007.
[5] K. Fujimoto, K. Asanuma, T. Wakabayashi, and T. Maeda, "Scale-model experiments on impedance and radiation efficiency measurements using scale-model human equivalent phantoms placed in the vicinity of the antenna under test," IEICE Technical Report, AP2008-83, Sept. 2008. (in Japanese)
[6] M. Danesh and J.R. Long, "Compact solar cell ultra-wideband dipole antenna," Proc. APS 2010, July 2010.
[7] A. Binder and R. Fachberger, "Wireless SAW temperature sensor system for high-speed high-voltage motors," IEEE Sensors Journal, vol.11, no.4, pp.966–970, April 2011.
[8] J. Sarrazin, Y. Mahe, S. Avrillon, and S. Toutain, "A new multimode antenna for MIMO systems using a mode frequency convergence concept," IEEE Trans. Antennas Propag., vol.59, no.12, pp.4481–4489, Dec. 2011.
[9] T. Chang and Y.D. Chen, "Tag antennas using differentially connected UC-PBG elements," Antennas Propagat. and EM Theory 2010, pp.353–355.
[10] P.H. Yang, Y. Li, L. Jiang, W.C. Chew, and T.T. Ye, "Compact metallic RFID tag antennas with a loop-fed method," IEEE Trans. Antennas Propag., vol.59, no.12, pp.4454–4462, Dec. 2011.
[11] D. Kim, T.W. Koo, J.I. Ryu, J.G. Yook, and J.C. Kim, "Accurate impedance measurement and implementation of a folded dipole antenna for RFID tags," Proc. ISAP 2009, pp.93–96, Oct. 2009.
[12] T. Koshinen, H. Rajagopalan, and Y. Rahmat-Samii, "Impedance measurements of various types of balanced antennas with the differential probe method," Proc. iWAT 2009, March 2009.
[13] X. Qing, C.K. Goh, and Z.N. Chen, "Impedance characterization of RFID tag antennas and application in tag co-design," IEEE Trans. Microw. Theory Tech., vol.57, no.5, pp.1268–1274, May 2009.
[14] L. Catarinucci, R. Colella, and L. Tarricone, "Design, development, and performance evaluation of a compact and long-range passive UHF RFID tag," Microw. and Optical Tech. Lett., vol.54, no.5, May 2012.
[15] M. Pigeon, R. D'Errico, and C. Delaveaud, "UHF-UWB tag antenna for passive RFID applications," Proc. EuCAP 2013, pp.3968–3972, April 2013.
[16] T. Fukasawa, H. Miyashita, and Y. Konishi, "Reduction of unbalanced current by a balun for an antenna measurement on a small radio," Proc. Commun. Conf. IEICE 2012, B-1-189, Sept. 2012. (in Japanese)
[17] K. Fujimoto and T. Maeda, "Input impedance measurement of antennas having asymmetric radiating elements with S-parameter method," Proc. Commun. Conf. IEICE 2007, B-1-178, Sept. 2007. (in Japanese)
[18] P.H. Yang, S. He, Y. Li, and L. Jiang, "Low-profile microstrip antenna with bandwidth enhancement for radio frequency identification applications," Electromagnetics, vol.32, pp.244–253, 2012.
[19] A.G. Alhaddad, R.A. Abd-Alhameed, D. Zhou, C.H. See, I.T.E. Elfergani, and P.S. Excell, "Low profile dual-band-balanced handset antenna with dual-arm structure for WLAN application," IET Microw. Antennas Propag., vol.5, no.9, pp.1045–1053, 2011.
[20] T. Sasamori, S. Watanabe, T. Tobana, and Y. Isota, "Calibration of measured impedance of balanced antenna by S-parameter method," Proc. IEICE Gen. Conf., B-1-129, March 2009. (in Japanese)
[21] T. Sasamori, T. Tobana, and Y. Isota, "Broadband measurement of input impedance using S-parameter method," IEICE Trans. Commun. (Japanese Edition), vol.J96-B, no.9, pp.1067–1075, Sept. 2013.
[22] T. Fukasawa, T. Yanagi, H. Miyashita, and Y. Konishi, "Extended S-parameter method including radiation pattern measurements of an antenna," IEEE Trans. Antennas Propag., vol.60, no.12, pp.5645–5653, Dec. 2012.
[23] R. Bourtoutian, C. Delaveaud, and S. Toutain, "Differential antenna design and characterization," Eucap 2009, pp.2398–2402, 2009.
[24] J. Hayakawa and N. Ishii, "Evaluation of balanced dipole antenna using balanced and unbalanced modes," IEICE Trans. Commun. (Japanese Edition), vol.J96-B, no.9, pp.1076–1085, Sept. 2013.
[25] T. Yanagi, T. Fukasawa, H. Miyashita, and Y. Konishi, "Measurement using the S-parameter method for radiation characteristics and mutual coupling of multiport antennas on a small ground," Proc. ISAP 2012, pp.1003–1006, Nov. 2012.
[26] N. Ishii, "Analysis of balanced and unbalanced modes for folded dipole antennas using mixed-mode S-parameter," Proc. Commun. Conf. IEICE 2013, B-1-222, Sept. 2013. (in Japanese)
[27] N. Ishii, "An extension of balanced and unbalanced mode analysis for balanced-fed asymmetric antennas," IEICE Technical Report, AMT2013-7, May 2013. (in Japanese)
[28] S.K. Kuo, S.L. Chen, and C.T. Lin, "An accurate method for impedance measurement of RFID tag antenna," Progress In Electromagnetics Research, vol.83, pp.93–106, 2008.
[29] J. Zhang, S. Pivnenko, and O. Breinbjerg, "A modified wheeler cap method for radiation efficiency measurement of balanced electrically small antennas," Proc. EuCAP 2010, April 2010.
[30] D.M. Pozer, Microwave Engineering, John Wiley & Sons, 2011.

Takayuki Sasamori was born in Hokkaido, Japan, on November 22, 1966. He received the B.E., M.E., and Ph.D. degrees in Electrical Engineering from Tohoku University, Sendai, Japan, in 1989, 1991, and 1994, respectively. In 1994, he was appointed Research Associate in the Department of Electrical and Communication Engineering, Tohoku University. From 1997 to 1999, he was an Assistant Professor at Sendai National College of Technology, Sendai, Japan. Currently, he is an Associate Professor in the Department of Electronics and Information Systems at Akita Prefectural University, Yurihonjo, Japan. His research interests include high-frequency asymptotic analysis of scattered waves, computational electromagnetics, antennas for mobile and personal communications, broadband antennas, and antenna measurements. He received the Young Engineer Award from IEICE Japan in 1997. Dr. Sasamori is a senior member of IEEE.

Toru Fukasawa was born in Tokyo, Japan, on December 24, 1969. He received a B.E., M.E. and Ph.D. degrees in electronic engineering from Hokkaido University, Sapporo, Japan, in 1992, 1994 and 2004, respectively. In 1994, he joined Mitsubishi Electric Corporation, Tokyo, Japan. His primary research activities are in small antenna analysis and measurement method. Dr. Fukasawa received the 2000 Young Engineer Award, the 2011 and 2012 Best Paper Awards of the Institute of Electronics, Information and Communication Engineers (IEICE). He is a member of IEEE.